

# EXPERIMENTS IN ACOUSTIC STRUCTURAL HEALTH MONITORING OF AIRPLANE PARTS

C. Tschöpe, E. Schulze, H. Neuniübel

M. Wolff, R. Schubert, R. Hoffmann

Fraunhofer Institute for  
Non-Destructive Testing  
Dresden Branch of IZFP

Technische Universität Dresden  
Laboratory of Acoustics and Speech Communication  
Matthias.Wolff@ias.et.tu-dresden.de

## ABSTRACT

In this preliminary study we investigate the application of statistical classifiers for structural health monitoring of materials commonly used in airplanes. Our approach is based on the propagation of ultrasonic guided waves through materials like aluminum or carbon fiber reinforced plastic (CFRP). When the material gets damaged, the sound propagation changes. There are two ways of detecting these changes: we can use a physical model of the wave propagation or we can use a statistical approach. In this paper we focus on the latter. We present results using classifiers based on Hidden Markov Models (HMM) and Support Vector Machines (SVM). We compare these results to acoustic travel time tomography as a representative of the physical model based methods.

**Index Terms**— Acoustic health monitoring, Hidden Markov models, Support vector machines, Acoustic tomography

## 1. INTRODUCTION

Aluminum and carbon fiber reinforced plastic (CFRP) are materials typically used for vital airplane construction elements like the fuselage, the wings and the empennage. During operation these parts may get damaged, for instance by impacting objects or fatigue. The risk of accidents caused by such damages may be reduced by a structural health monitoring. One possibility to do this is sending ultrasonic impulses through the material and recording the induced ultrasound through a network of sensors. If some structural damage occurs, the sound propagation through the material will change. By recognizing such changes we can detect structural damages.

In this preliminary study we experimented with two test objects, an aluminum plate and a CFRP plate. We artificially introduced defined structural damage and tried to detect it. Sections 1.1 and 1.2 describe the test objects and setup, section 2 introduces the investigated health monitoring methods and, finally, section 3 presents first results.

### 1.1. Test Object A - Aluminum Plate

An aluminum plate of  $1000 \times 1000 \times 2.5$  mm is the first test object. It is clamped at its corners and instrumented with 8 ultrasound transducers<sup>1</sup> (A1 ... D2) which are glued to its

<sup>1</sup>senders/receivers

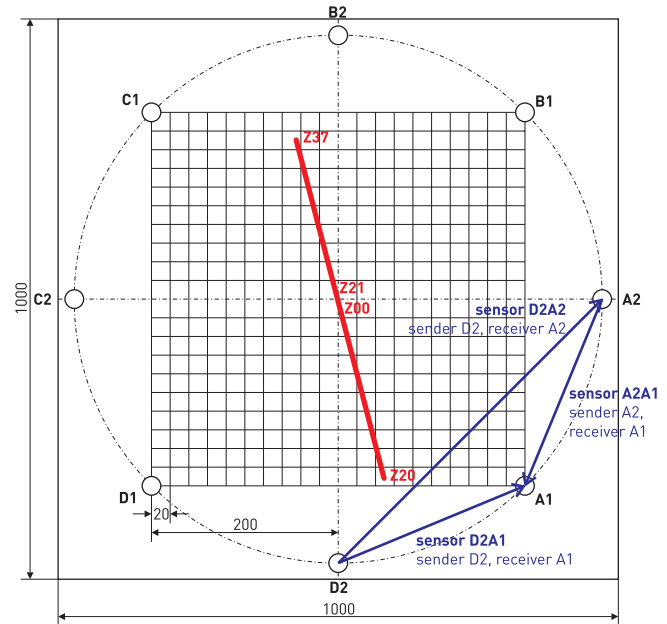


**Fig. 1.** Sketch of test object A (aluminum plate, not to scale). The small circles denote the positions of ultrasonic actuators, the thick line denotes the position of an artificially introduced fissure (in 1 cm steps center to bottom, then center to top).

surface forming a circle of 570 mm in diameter (see Fig. 1). At the beginning of the experiment the plate is intact (damage state Z00). Then a fissure of increasing length from 1 through 37 cm is artificially introduced (thick line in Fig. 1; damage states Z01 – Z37). In each state the guided wave propagation through the plate is measured by sending a defined ultrasonic impulse subsequently through each transducer and recording the sound waves arriving at the others. For better legibility we call one sender/receiver combination a *sensor*. Thus we have  $8 \times 7 = 56$  “sensors”<sup>2</sup>.

### 1.2. Test Object B - CFRP Plate

The second test object is a CFRP plate of  $860 \times 600 \times 5$  mm. The plate was instrumented with 12 ultrasonic actuators ar-

<sup>2</sup>the sending unit does not record its own sound

ranged in a regular grid of 4 columns and 3 rows as shown in Fig. 2. At the beginning of the experiment the plate was intact (damage state Z00). Then it was increasingly damaged by introducing impacts using a steel hemisphere of 2.1 kg weight (damage states Z01 – Z05). Table 1 lists the impacts, their energies and the investigated states of the CF plate. The positions of the impacts are shown in Fig. 2. The measurement procedure is exactly as described in section 1.1. There are  $12 \times 11 = 132$  “sensors”.

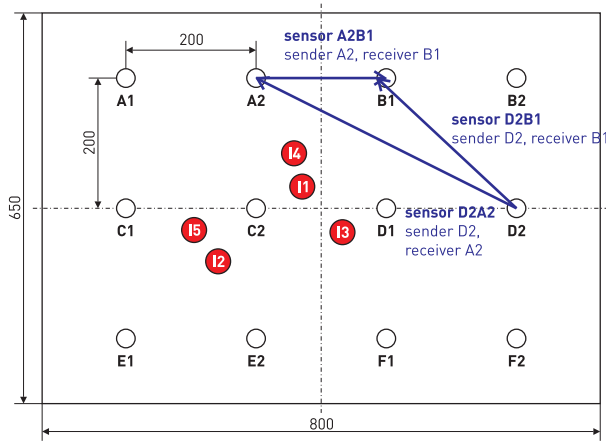


**Fig. 2.** Sketch of test object B (CFRP plate). The white circles denote the positions of the ultrasonic actuators, the dark ones the positions of artificially introduced impacts.

| Impact | Energy | Back of plate ... | State | Impacts         |
|--------|--------|-------------------|-------|-----------------|
|        |        |                   | Z00   | none            |
| I1     | 15 J   | supported         | Z01   | I1              |
| I2     | 25 J   | supported         | Z02   | I1, I2          |
| I3     | 45 J   | supported         | Z03   | I1, I2, I3      |
| I4     | 25 J   | free              | Z04   | I1, I2, ..., I4 |
| I5     | 25 J   | free              | Z05   | I1, I2, ..., I5 |

**Table 1.** List of artificially introduced impacts to test object B. There are two types: on impacts I1 ... I3 the plate rested flatly on a pad, on impacts I4 and I5 the plate rested on a frame and its back was not supported. The latter impacts caused much greater damage than the first ones.

## 2. NON-DESTRUCTIVE TESTING METHODS

From the test setup described in section 1 we obtain a set of signal files per sensor and per damage state. We have two possibilities of processing these signals: we can use a physical model of the wave propagation or a statistical approach which tries to classify the damage state from the signal characteristics without any prior knowledge. One technique representing the first strategy is described in section 2.1. This approach allows one to locate the damage but it may get computationally expensive for complex structures. The second strategy is described in section 2.2. It is simpler, somewhat more sensible in detecting damages but not capable of locating them.

### 2.1. Acoustic Tomography

Acoustic travel time tomography (see e.g. [1, 2]) is a standard technique in non-destructive testing. It creates an image of the discrete distribution of Lamb wave velocities  $V_L$  in the scanned region. These waves are induced by ultrasonic sound actuators as described in section 1.1. Tomographic image reconstruction requires a uniform and dense coverage of the scanned area with sound rays and as many as possible travel time measurements between senders and receivers. We used a straight-line sound ray model which will, in our application, not give a precise image of the damage but is still sufficient to roughly locate it. We chose this method because it is quicker and requires less computational power. Using the geometry displayed in Fig. 1 we accomplished an image resolution of  $40 \times 40$  mm using the damped SIRT reconstruction. Fig. 3 shows the reconstructed image of damage state Z16 (fissure of 16 cm length). In our experiments, acoustic travel time tomography was able to detect and locate fissures from 12 cm up.

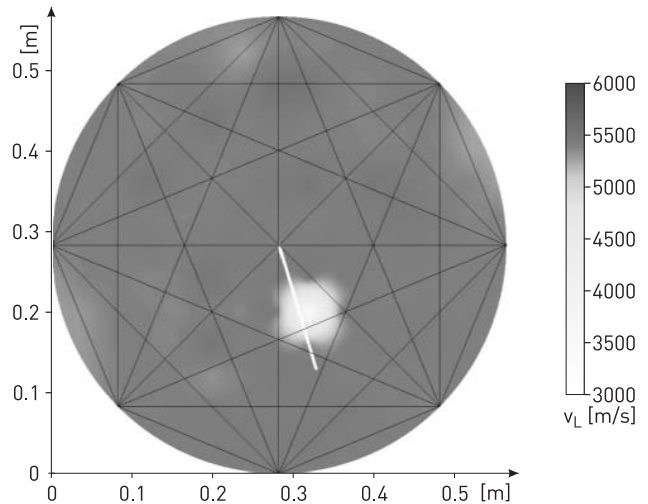


**Fig. 3.** Lamb wave velocity ( $V_L$ ) image obtained by the damped SIRT. The actual damage is indicated by the white line.

### 2.2. Statistical Classifiers

Statistical classifiers have been successfully applied to non-destructive testing (e.g. [3, 4]). They usually transform the input signals into sequences of observation vectors – “the observation” – before processing them. We used a fairly coarse short-term auto power spectrogram as feature extraction. The details are summarized in table 2.

#### Hidden Markov Model (HMM) Classifier

As is well known, HMMs model signals by a sequence of “states” interpreted as sort of signal “events”. They use (mostly Gaussian) probability density functions to model these states in combination with a finite state grammar on their succession. Using the Viterbi algorithm we can compute the neglog.

|            |                    | Test object    |         |
|------------|--------------------|----------------|---------|
|            |                    | A              | B       |
| Setup      | # Damage states    | 38             | 8       |
|            | # Sensors          | 56             | 132     |
|            | # Signals          | 532,000        | 792,000 |
| Excitation | Type               | Ricker wavelet |         |
|            | Center frequency   | 250 kHz        | 100 kHz |
| Recording  | Sampling frequency | 6.25 MHz       |         |
| Features   | Type               | short-term APS |         |
|            | Dimension          | 24             |         |
|            | Vectors/signal     | 48             | 106     |

**Table 2.** Experimental setup

likelihood  $NLL$  that a given observation comes from a particular HMM. The  $NLL$  may serve as a measure how well that HMM fits the observation.

For both test objects we trained one HMM per damage state *and* sensor from 80 % of the recorded material. The remaining data were classified by these models. We used three-state forward connected HMMs with exactly one Gaussian PDF with full covariance matrix per state (we also tested mixture Gaussians but they did not help very much). The test signals were classified using the following two strategies:

- **HMM/m** – Identify a particular damage state by computing the  $NLL$  of each HMM and deciding for the damage class whose HMM yields the smallest  $NLL$ .
- **HMM/s** – Only compute the  $NLL$  of the intact state’s HMM and decide by a threshold whether the observation comes from the intact or the damaged object. We can use the  $NLL$  value to quantify the degree of damage.

HMM/s is the more realistic approach as it does not require models of damages which might be difficult to obtain.

### Support Vector Machine (SVM) Classifier

SVMs are capable of classifying vectors of huge dimension. However, they are not suitable for vector *sequences* unless they are all of the same length. Fortunately in our task this is the case (see table 2). Here we can simply concatenate all observation vectors of one signal to a super vector.

We used a soft-margin SVM with a simple linear kernel. As for the HMMs we trained one SVM for each damage state *and* sensor using the same data sets. Because these sets are huge we applied the incremental training method by Domeniconi et al. [5]. We employ a one-against-one multi-class SVM [6] and use the same two strategies as with the HMMs:

- **SVM/m** – Identify a particular damage state.
- **SVM/s** – Compute the distance to intact state’s model.

For the SVM/s classifier we only compute a probability of test vectors belonging to the intact class. This can be done according to [7]. To present comparable results we state the negative logarithmic probabilities ( $NLP$ ) in section 3. In contrast

to the HMM classifier, this version of the SVM does not only use information on the intact class but also on all other (damage) classes. So the comparison between SVM and HMM in section 3 is not quite fair as it favors the SVMs.

### Sensor Fusion

As signals originating from different sensors may have different characteristics we cannot model them altogether in one HMM or SVM unless we would build even larger super vectors. With over a hundred sensors this quickly gets unfeasible. Therefore we decided to train separate models for *each* sensor. Hence the classifiers come up with whole vector of likelihoods for each test recording. We would like to fuse the individual likelihoods to enhance the result. There are sophisticated sensor fusion strategies (e.g. [8]). However, we found the following two very simple ones absolutely sufficient for our problem:

- $\overline{NLx}$  – Compute the mean  $NLL$  or  $NLP$ .
- **GSS<sub>n</sub>** – Do a PCA on a development set of  $NLL$  or  $NLP$  vectors, clip the transformed vectors to  $n$  components, estimate one Gaussian PDF and compute the neglog. probability density of the test vectors.

## 3. EXPERIMENTAL RESULTS

The results presented in the following were obtained with the statistical classifiers described in section 2.2. For comparison section 2.1 contains results of the acoustic tomography.

### Damage Detection

First we use the single-model classifiers HMM/s and SVM/s together with the naïve sensor fusion methods  $\overline{NLx}$  and  $GSS_n$  (all described in section 2.2). These classifiers decide for each test signal whether it comes from an intact or damaged object. In case of errors they may either mistakenly classify an intact signal as a damage (false rejection) or vice versa (false acceptance). The performance of such systems is assessed by a receiver operating characteristics (ROC) curve. A significant point on this curve is the equal error rate ( $EER$ ) where there are as many false rejections as false acceptances. If  $EER = 0$  the classifier does perfectly. In such a case we additionally consider a classification safety margin:

$$CM = \frac{\min(X_{\text{damaged}}) - \max(X_{\text{intact}})}{\text{mean}(X_{\text{damaged}}) - \text{mean}(X_{\text{intact}})}$$

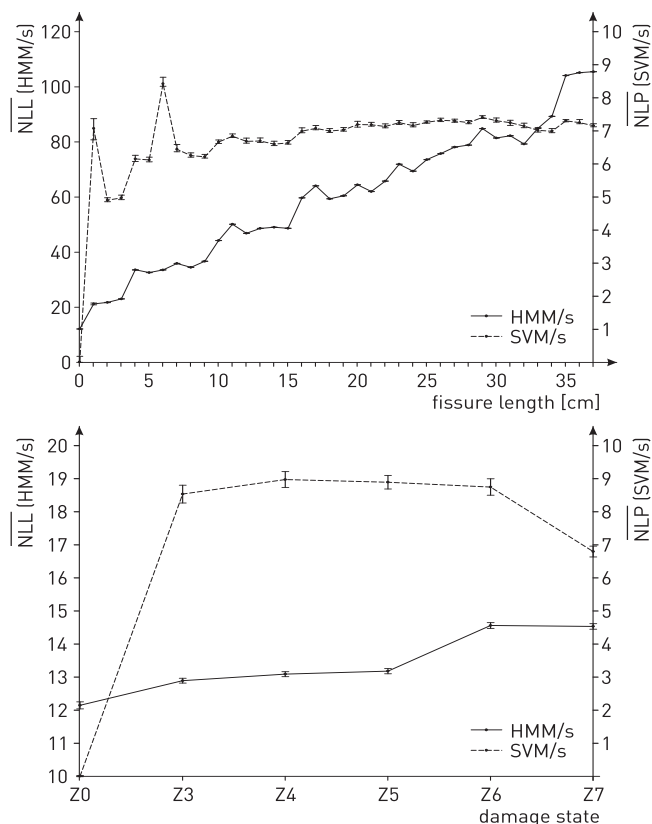
where  $X$  denotes the set of  $\overline{NLx}$  or  $GSS_n$  scores computed by the sensor fusion.

Table 3 shows that in our test the SVM/s classifier always does perfectly and has comfortable safety margins. With  $EER$ s of less than 1 % the HMM/s classifier performs very well, too. Even though a little less accurate, the HMM classifier has got its advantage: it provides a better clue to the degree of damage. Fig. 4 shows the means and standard deviations of the  $\overline{NLx}$  scores over the damage states. While the

|      | HMM/s            |         |     | SVM/s            |         |     |
|------|------------------|---------|-----|------------------|---------|-----|
| Test | $EEER$ [%]       |         |     |                  |         |     |
| Obj. | $\overline{NLx}$ | $GSS_n$ | $n$ | $\overline{NLx}$ | $GSS_n$ | $n$ |
| A    | 0.2              | 0.0     | 2   | 0.0              | 0.0     | 2   |
| B    | 0.3              | 1.0     | 16  | 0.0              | 0.0     | 2   |
|      | $CM$ [%]         |         |     |                  |         |     |
| A    | —                | 11.1    | 2   | 73.7             | 96.8    | 2   |
| B    | —                | —       | 16  | 88.6             | 94.3    | 2   |

**Table 3.** Damage detection performance of the single-model classifiers with sensor fusion, measured as equal error rate and, if  $EEER = 0$ , as classification margin  $CM$ .

SVM classifier merely detects that there is some damage but is inconclusive on its severity, the HMM classifier computes scores which correlate with the degree of damage.



**Fig. 4.** Means and standard deviations of the  $\overline{NLx}$  scores per damage state for test objects A (top) and B (bottom).

#### Identification of Individual Damage States

Table 4 shows that the multi-model versions HMM/m and SVM/m of both classifiers are also capable of *identifying* particular damage states. In this setup we let the classifiers decide for one state  $Z_{xx}$  (instead of just for “intact” or “damaged”) and count how often they fail therein (error rate  $ER$ ). To make

the task even harder, we do not use sensor fusion. Each decision is based on a *single* sensor. We state the minimal, maximal and mean error rates over all sensors. In our test SVMs again clearly outperform the HMMs. Considering the fact that the acoustic tomography (which uses *all* sensors) did not detect fissures shorter than 12 cm in object A at all, the performance of the HMMs is still remarkable.

|        | HMM/m    |      |             | SVM/m |     |            |
|--------|----------|------|-------------|-------|-----|------------|
| Test   | $ER$ [%] |      |             |       |     |            |
| Object | min      | max  | mean        | min   | max | mean       |
| A      | 0.0      | 9.8  | <b>2.0</b>  | 0.0   | 2.0 | <b>0.3</b> |
| B      | 2.2      | 26.7 | <b>12.1</b> | 0.0   | 3.1 | <b>0.6</b> |

**Table 4.** Damage identification performance of the multi-model classifiers without sensor fusion, measured as error rate  $ER$

#### 4. CONCLUSION

We tested statistical classifiers for acoustic structural health monitoring of aluminum and CFRP components and compared their performance to acoustic travel time tomography. Both, HMM and SVM classifiers, securely detect all investigated damages and showed a greater sensibility than the tomography. However, the statistical approaches do not allow a localization of damages as tomography does.

#### 5. REFERENCES

- [1] A.C. Kak and M. Slaney, “Principles of computerized tomographic imaging,” *IEEE Press*, 1988.
- [2] F. Schubert, “Basic principles of acoustic emission tomography,” *Journal of Acoustic Emission*, vol. 22, pp. 147–159, 2004.
- [3] H. Y. K. Lau, “A hidden markov model-based assembly contact recognition system,” *Mechatronics*, vol. 13(8-9), pp. 1001—1023, 2003.
- [4] C. Tschöpe et al., “Classification of non-speech acoustic signals using structure models,” in *Proc. IEEE ICASSP*, 2004, pp. 653–656.
- [5] C. Domeniconi and D. Gunopulos, “Incremental Support Vector Machine construction,” in *IEEE International Conference on Data Mining*, 2001, pp. 589–592.
- [6] C.-W. Hsu et al., “A comparison of methods for multi-class Support Vector Machines,” *IEEE Transactions on Neural Networks*, vol. 13, no. 2, pp. 415–425, 2002.
- [7] C.-J. Lin T.-F. Wu and R. C. Weng, “Probability estimates for multi-class classification by pairwise coupling,” *Machine Learning Research*, vol. 5, pp. 975–1005, 2004.
- [8] D. Hall, *Mathematical Techniques in Multisensor Data Fusion*, Artech House, Boston, London, 1992.